

# FEAST YOUR EYES: MIXTURE-OF-RESOLUTION ADAPTATION FOR MULTIMODAL LARGE LANGUAGE MODELS

Gen Luo<sup>1,2</sup>, Yiyi Zhou<sup>1</sup>, Yuxin Zhang<sup>1</sup>, Xiawu Zheng<sup>1</sup>, Xiaoshuai Sun<sup>1</sup>, Rongrong Ji<sup>1</sup>✉

<sup>1</sup>Key Laboratory of Multimedia Trusted Perception and Efficient Computing,  
Ministry of Education of China, Xiamen University, 361005, P.R. China.

<sup>2</sup>OpenGVLab, Shanghai AI Laboratory.

## ABSTRACT

In existing multimodal large language models (MLLMs), image resolution plays a significant role for granular visual recognition. However, directly increasing image resolution leads to expensive computational cost for MLLMs. In this paper, we reveal that a combination of low- and high-resolution visual features can efficiently mitigate this shortcoming. Based on this principle, we propose a novel and efficient method for MLLMs, termed *Mixture-of-Resolution Adaptation* (MRA). In particular, MRA adopts two visual pathways for images of different resolutions, where high-resolution visual information is embedded into the low-resolution pathway via the novel *mixture-of-resolution adapters* (MR-Adapters). This design also greatly reduces the input sequence length of MLLMs. To validate MRA, we apply it to a recent MLLM called LLaVA, and term the new model *LLaVA-HR*. We conduct extensive experiments on 17 vision-language (VL) tasks, which show that LLaVA-HR outperforms existing MLLMs on 15 VL tasks, *e.g.*, +5.2% on TextVQA. More importantly, both training and inference of LLaVA-HR remain efficient with MRA, *e.g.*, **20 training hours** and **faster inference speed** than LLaVA-NeXT. Source codes are released at: LLaVA-HR.

## 1 INTRODUCTION

Driven by the remarkable success of large language models (LLMs) (Touvron et al., 2023; Chen et al., 2020), research on multi-modal large language models (MLLMs) also receives an influx of interest in both academia and industry (Liu et al., 2023b; Luo et al., 2023; Alayrac et al., 2022; Chen et al., 2022; 2023c). Numerous efforts have been recently devoted to extending LLMs to more modalities, achieving breakthroughs on various vision-language tasks (Goyal et al., 2017; Singh et al., 2019; Hudson & Manning, 2019). Despite their success, existing MLLMs still fall short of granular visual recognition. For instance, the powerful GPT4-V also suffers from visual hallucinations when identifying small and occluded objects (Tong et al., 2024). This shortcoming inevitably limits the practical use of MLLMs.

To compensate for this shortcoming, early practitioners often resort to scaling up model size and increasing per-training data size (Alayrac et al., 2022; Li et al., 2023b; Bai et al., 2023). For instance, InstructBLIP (Dai et al., 2023) adopts over 129M image-text pairs for vision-language (VL) alignments, showing that a larger visual encoder is beneficial for MLLMs. Similarly, Qwen-VL (Bai et al., 2023) also increases the parameters of visual encoder to 1.9 billion and uses 1.5 billion image-text pairs for pre-training. Despite effective, this paradigm is prohibitively expensive, which often consumes about thousands of GPU hours.

Orthogonal to these works, we study the visual shortcoming of MLLMs from the perspective of image resolutions. As revealed in previous VL research (Jiang et al., 2020; Tong et al., 2024), increasing the resolution of input images is a straightforward solution for visual recognition, which becomes more important for MLLMs that involve fine-grained visual reasoning (Rose et al., 2023). As shown

✉Corresponding author.

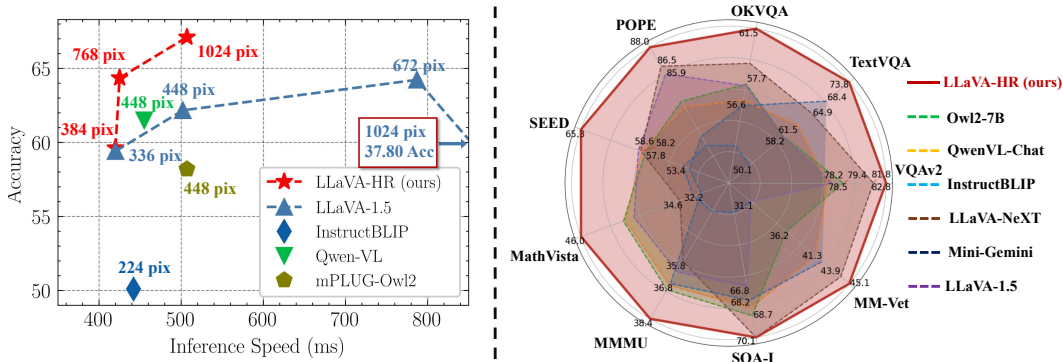


Figure 1: Comparison between existing MLLMs and LLaVA-HR on TextVQA (left) and various benchmarks (right). Increasing image resolution is effective yet expensive for fine-grained visual understanding. In contrast, LLaVA-HR can efficiently adapt high resolution to boost performance.

in Fig. 1, increasing the resolution of LLaVA-1.5 (Liu et al., 2023a) from  $384 \times 384$  to  $672 \times 672$  can bring obvious performance gains (+4.6%) on TextVQA (Singh et al., 2019). However, the use of high-resolution images will greatly exacerbate the already high computational cost of MLLMs. For instance,  $448 \times 448$  resolution will increase the computation complexity of LLaVA by about 1.4 times compared with the default  $336 \times 336$ . In addition, the training will become unstable as the resolution is greatly increased<sup>1</sup>, e.g., a sharp drop at  $1,022 \times 1,022$  resolution in Fig. 1. Although such an issue can be overcome by dividing high-resolution images into small patches via the dynamic slicing strategy Liu et al. (2024a), its computational cost still remains expensive for MLLMs.

In this paper, we focus on the efficient high-resolution image adaptation of MLLMs and propose a novel method called *mixture-of-resolution adaptation* (MRA). As shown in Fig. 2, MRA adopts an innovative dual visual pathway design to process the input images of high- and low-resolutions simultaneously. Specifically, one pathway aims to encode global information of low-resolution images, while the other one serves to capture fine-grained semantics from high-resolution images. Meanwhile, these two pathways are closely interacted via the novel *mixture-of-resolution adapters* (MR-Adapters), which embeds the high-resolution visual information into the low-resolution modeling. In this way, we can use a much fewer number of visual tokens to represent the input images from macro- to micro-views. With the careful design of dual-pathway structure, MRA can easily scale the image resolution up to  $1,024 \times 1,024$  pixels while maintaining high efficiency.

To validate MRA, we apply it to a recent MLLM called LLaVA (Liu et al., 2023b;a), and term the new model as LLaVA-HR. We conduct extensive experiments on 17 vision-language (VL) tasks, including common VL tasks like VQAv2 (Goyal et al., 2017) and MLLM benchmarks such as POPE (Li et al., 2023c). Experimental results show that LLaVA-HR outperforms existing MLLMs on 15 of 17 VL tasks, e.g., +9.6% over LLaVA-1.5 on TextVQA. More importantly, the training and inference of LLaVA-HR are cost-effective. In particular, the pre-training and instruction tuning of LLaVA-HR (7B,  $1,024 \times 1,024$ ) only take a total of 20.7 hours on 8 A800 GPUs, which is *hundreds of times cheaper* than InstructBLIP (Dai et al., 2023) and Qwen-VL (Bai et al., 2023). Under the same high-resolution setting, its inference speed is *consistently faster* than LLaVA-1.5 (Liu et al., 2023a) and LLaVA-Next Liu et al. (2024a).

In summary, our contributions are three folds:

- We propose a novel and efficient adaptation scheme, termed *mixture-of-resolution adaptation* (MRA), which adopts a novel dual visual pathway design to obtain the benefits of high-resolution visual information while keeping training and inference efficient.
- We propose a novel *mixture-of-resolution adapter* (MR-Adapter) for MRA, which can embed the high-resolution information into the low-resolution visual pathway to improve visual descriptive power.
- Based on MRA, we propose a powerful MLLM, coined LLaVA-HR, which outperforms existing MLLMs on 15 of 17 VL tasks and are much more efficient than most MLLMs.

<sup>1</sup>Visual encoders like CLIP-ViT are pre-trained with low resolution, and the significant increase of resolution may hurt feature representations.

## 2 RELATED WORK

### 2.1 MULTIMODAL LARGE LANGUAGE MODELS

Driven by the great successes of large language models (LLMs) (Gilardi et al., 2023; Touvron et al., 2023; Chen et al., 2020), growing interest has been aroused in building end-to-end multimodal large language models (MLLMs) (Liu et al., 2023b; Zhu et al., 2023; Luo et al., 2023; Bai et al., 2023; Fuyu-8B, 2023; Peng et al., 2023; Luo et al., 2024a;b). In particular, most existing MLLMs adopt a modular structure (Luo et al., 2023; Liu et al., 2023b), which utilizes an intermediate network to project the visual features into the word embedding space of the LLM. Then, the LLM is used to accomplish various VL tasks in an autoregressive manner. Based on the modular structure, existing MLLMs can be distinguished by the designs of the intermediate network. Popular MLLMs represented by LLaVA (Liu et al., 2023b) often adopt a linear projection layer or an MLP layer to connect the visual encoder and the LLM (Liu et al., 2023b; Chen et al., 2023a;c; Peng et al., 2023). The other works employ sampler-based modules to bridge the gap between the visual encoder and the LLM (Bai et al., 2023; Alayrac et al., 2022; Li et al., 2023b). These sampler-based modules can effectively reduce the number of visual tokens, but often requires a large-scale pre-training to achieve a promising performance (Bai et al., 2023; Li et al., 2023b). Despite the effectiveness, the low-resolution visual perception still limits the performance of existing MLLMs in fine-grained tasks.

### 2.2 HIGH-RESOLUTION MULTIMODAL LARGE LANGUAGE MODELS

To improve the perception ability of MLLMs, increasing attentions have been focused on high-resolution MLLMs (Liu et al., 2024a; Li et al., 2024c; Liu et al., 2024b; Li et al., 2024b; Chen et al., 2024b). Among them, most methods (Li et al., 2024c; Liu et al., 2024a) adopt the dynamic slicing strategy to divide a high-resolution image into multiple low-resolution patches. By doing so, pre-trained visual encoders can maintain their default resolutions for adapting high-resolution processing, and support images with flexible aspect ratio. For example, Monkey (Li et al., 2024c) and LLaVA-Next (Liu et al., 2024a) divide input images into a set of  $448 \times 448$  patches for high-resolution visual understanding. Based on this framework, Chen et al. (2024b) and Dong et al. (2024) further explore the strategy to realize the optimal image division. Despite the effectiveness, their computational cost is still expensive as the image resolution increases. Orthogonal to these works, we aim to improve image resolution in an efficient way, which still lacks extensive explorations.

### 2.3 VISUAL REPRESENTATIONS FOR MULTIMODAL LARGE LANGUAGE MODELS

The pursuit of better visual representations has been a popular research trend in the VL community (Lu et al., 2019; Jiang et al., 2020; Radford et al., 2021). Early endeavors mainly explore the object-level features for VL models (Lu et al., 2019; Zhang et al., 2021). Driven by the large-scale image-text pre-training, grid features from CLIP (Radford et al., 2021) have demonstrated the great efficiency and generalization in MLLMs (Liu et al., 2023b; Chen et al., 2022; Alayrac et al., 2022). Based on grid features, existing researchers mainly improve visual representations by scaling up the visual encoder. For example, PaLI (Chen et al., 2022) increases the parameters of visual encoder to 3 billions and shows the significant performance boost of MLLMs. In contrast to these works, we improve the visual representations for MLLMs from the perspective of dual-branch network interactions, and propose a novel and efficient solution, namely mixture-of-resolution adaptation.

## 3 PRELIMINARY

We first recap the structure of multimodal large language models (MLLMs), which consists of an image encoder  $\mathcal{F}_{\mathcal{I}}(\cdot)$ , an intermediate network  $\mathcal{F}_{\mathcal{P}}(\cdot)$  and an LLM  $\mathcal{F}_{\mathcal{L}}(\cdot)$ .

In particular, given an input image  $I \in \mathbb{R}^{H \times W \times 3}$  and a textual instruction  $T \in \mathbb{R}^L$ , the visual tokens  $\mathbf{F}_v \in \mathbb{R}^{(h \times w) \times d}$  are obtained via the image encoder, and the text tokens  $f_t \in \mathbb{R}^{l \times d}$  are represented by the corresponding word embeddings. Based on the visual and textual tokens, the LLM will decode the target word step by step, formulated as

$$p_t = \prod_{s=1}^{S+1} \mathcal{F}_{\mathcal{L}}(R_s | \mathcal{F}_{\mathcal{P}}(\mathbf{F}_v), f_t, R_{0:s-1}). \quad (1)$$

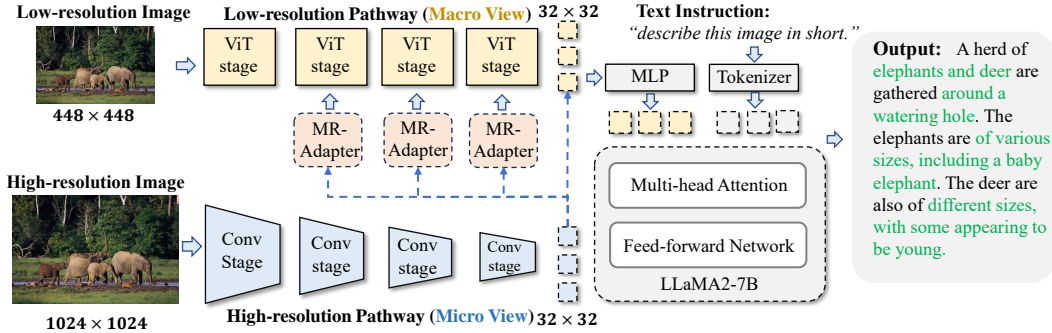


Figure 2: **Illustration of Mixture-of-Resolution Adaptation (MRA) and its deployment on LLaVA-HR.** MRA employs dual visual pathways to process high-resolution and low-resolution images, respectively. High-resolution information is embedded into the fast pathway via a novel mixture-of-resolution adapter (MR-Adapter).

Here,  $p_t \in \mathbb{R}^m$  denotes the probabilities of the predicted word and  $m$  is the size of word vocabulary.

In some MLLMs (Liu et al., 2023b;a),  $\mathcal{F}_{\mathcal{P}}(\cdot)$  is often a stack of simple linear layers, which are used to directly project the visual tokens onto the semantic space of LLMs. Although simple and effective, this strategy inevitably leads to a longer visual sequence as the resolution increases, e.g., 5,329 tokens for  $1,022 \times 1,022$  resolution in LLaVA-1.5. In practice, processing such a large number of tokens is computationally expensive in MLLMs. To further reduce the number of visual tokens, recent advances adopt the sampler-based module for  $\mathcal{F}_{\mathcal{P}}(\cdot)$ , e.g., *QFormer* (Li et al., 2023b), which aggregates visual features into several query tokens that LLM can directly handle. Nevertheless, these methods often require large-scale pre-training to achieve VL alignments (Bai et al., 2023).

Based on the above analyses, we conclude that the main difficulty of high-resolution image adaptation lies in the rapidly growing visual sequence. This issue motivates us to further explore how to efficiently encode richer visual information with fewer visual tokens.

## 4 MIXTURE-OF-RESOLUTION ADAPTATION

### 4.1 OVERVIEW

To address the above issues, we propose a novel and efficient method for MLLMs, termed *mixture-of-resolution adaptation* (MRA). As shown in Fig. 2, MRA aims to embed high-resolution information into the low-resolution one via a dual pathway design. In this case, MRA can keep a smaller number of visual tokens while encoding richer visual information.

In particular, given the input images of two resolutions  $I_l \in \mathbb{R}^{H_l \times W_l \times 3}$  and  $I_h \in \mathbb{R}^{H_h \times W_h \times 3}$ , the process of MRA can be formulated as

$$\mathbf{F}_v = \mathcal{F}_{\mathcal{I}_l}(I_l, \mathcal{F}_{\mathcal{A}}(\mathbf{F}_{vh}; \theta_{\mathcal{A}}); \theta_{\mathcal{I}_l}), \quad (2)$$

where  $\mathbf{F}_{vh} = \mathcal{F}_{\mathcal{I}_h}(I_h; \theta_{\mathcal{I}_h})$ .

Here,  $\mathbf{F}_{vh} \in \mathbb{R}^{h_h \times w_h \times d_h}$  and  $\mathbf{F}_v \in \mathbb{R}^{h \times w \times d}$  denote the high-resolution features and the final visual features, respectively. And  $\mathcal{F}_{\mathcal{I}_l}(\cdot)$  and  $\mathcal{F}_{\mathcal{I}_h}(\cdot)$  are the visual encoders for high-resolution and low-resolution images, respectively.  $\mathcal{F}_{\mathcal{A}}$  denotes the *mixture-of-resolution adapter* (MR-Adapter). Based on Eq. 2, the obtained visual features will be further processed by the LLM based on Eq. 1.

### 4.2 DUAL VISUAL PATHWAYS

As shown in Fig. 2, dual visual pathways, i.e.,  $\mathcal{F}_{\mathcal{I}_l}(\cdot)$  and  $\mathcal{F}_{\mathcal{I}_h}(\cdot)$  are the key design of MRA. To maximize their benefits, we consider the heterogeneous dual-branch design from two aspects.

**Visual functionality.** Firstly, the dual visual pathways process images from macro- and micro-views, which is inspired by the visual system of human being (Merigan & Maunsell, 1993; Robertson & Lamb, 1991). Particularly, Robertson & Lamb (1991) find that the visual system processes local

and global semantics via different pathways. Similar mechanisms in computer vision are not new. Previous works (Chen et al., 2021; Peng et al., 2021) like CrossViT (Chen et al., 2021) typically incorporate this feature into their network design for image classification.

However, the exploration of dual visual pathways in high-resolution adaptation for MLLMs can still bring new insights beyond previous works, *i.e.*, fewer visual tokens can also result in stronger visual understanding. Specifically, one visual pathway aims to capture fine-grained semantics from high-resolution images *i.e.*, processing images from local view. The other pathway is designed to encode global information from low-resolution images for a larger receptive field. In this case, MRA can not only efficiently process high-resolution images, but also greatly benefits from two complementary visual semantics.

**Visual alignment.** The alignment of two pathways is also challenging in MLLMs, which typically requires additional fusion layers like cross-attentions (Vaswani et al., 2017). Due to different resolutions, these two pathways often produce visual features of different shapes, impeding their quick alignments (Yu et al., 2019). To overcome this limitation, we adopt different downsampling rates for the low- and high-resolution pathways, respectively. Thus, their output features can keep the same spatial shape.

Based on the above motivations,  $\mathcal{F}_{\mathcal{I}_l}(\cdot)$  and  $\mathcal{F}_{\mathcal{I}_h}(\cdot)$  are designed as a vision transformer (ViT) (Dosovitskiy et al., 2020) and a convolutional network (CNN) (Liu et al., 2022), respectively. Specifically, CNN is equipped with a downsampling stride of 32 to process high-resolution images. ViT encodes low-resolution images with a downsampling stride of 14. Notably, such designs also ensure the efficiency of MLLMs, where the high-resolution images are processed by the efficient CNN, and the number of visual tokens is also kept small via the large downsampling stride.

### 4.3 MIXTURE-OF-RESOLUTION ADAPTER

To better collaborate the feature learning of two pathways, we propose a *mixture-of-resolution adapter* (MR-Adapter) to embed high-resolution information of CNN into different stages of ViT. This early fusion strategy can leverage ViT’s deep Transformer layers to excavate fine-grained context from different visual sources.

In particular, given the visual features  $\mathbf{F}_{vh} \in \mathbb{R}^{h \times w \times d_h}$  of the a high-resolution image, we embed them into the low-resolution visual pathway by

$$\mathbf{F}_{vl}^i = \mathcal{F}_l(\mathbf{F}_{vl}^i; \theta_l) + g \cdot \mathcal{F}_h(\mathbf{F}_{vh}; \theta_h). \quad (3)$$

Here,  $\mathbf{F}_{vl}^i \in \mathbb{R}^{h \times w \times d_l}$  are features from the *i*-th stage of ViT.  $\mathcal{F}_l(\cdot)$  is a lightweight convolution layer with a residual connection.  $\mathcal{F}_h(\cdot)$  denotes an MLP layer.  $g$  is a dynamic score to control the weights of high-resolution information, defined by

$$g = \delta(W_2 \sigma(W_1 f_v)). \quad (4)$$

Here,  $f_v \in \mathbb{R}^{2d}$  is the global average pooling of visual features  $[\mathcal{F}_l(\mathbf{F}_{vl}^i), \mathcal{F}_h(\mathbf{F}_{vh})]$ , where  $[\cdot]$  denotes the concatenation operation.  $W_1 \in \mathbb{R}^{2d \times \frac{d}{2}}$  and  $W_2 \in \mathbb{R}^{\frac{d}{2} \times d}$  are two projection matrices.  $\sigma$  and  $\delta$  denote the activation function of *GELU* and *Tanh*, respectively.

As shown in Fig. 2, high-resolution information can be fused with the features in each block of ViT. In this case, the low-resolution features of ViT also contain rich semantics, improving the visual descriptive power of MLLMs.

### 4.4 THE DEPLOYMENT ON MLLM

We apply MRA to LLaVA-1.5 (Liu et al., 2023a) and construct a new model, namely LLaVA-HR. Its training consists of two stages, *i.e.*, low-resolution pre-training and high-resolution instruction tuning.

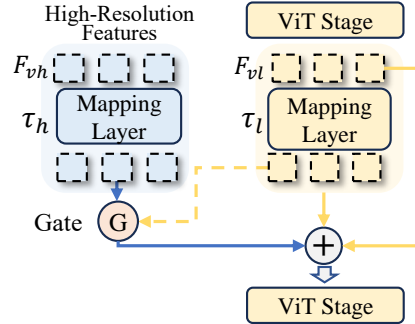


Figure 3: **Illustration of MR-Adapter.** MR-Adapter can dynamically embed the high-resolution features into the low-resolution pathway.

**Stage 1: Low-resolution pre-training.** Similar to LLaVA (Liu et al., 2023b) and LLaVA-1.5 (Liu et al., 2023a), this stage aims to optimize the projector to align the visual features with the word embedding space of LLM. Therefore, the image encoder and the LLM are frozen during pre-training. Besides, we adopt low resolutions for two pathways, *i.e.*,  $384 \times 384$  and  $336 \times 336$ . In this stage, the MR-Adapter is not inserted, and output features of dual pathways are upsampled to the same size and directly combined.

**Stage 2: High-resolution instruction tuning.** During instruction tuning, we increase the resolution of the high-resolution pathway, *e.g.*, from  $384 \times 384$  to  $1,024 \times 1,024$ . And the low-resolution one is also accordingly adjusted to ensure the visual alignment of two pathways, *e.g.*, from  $336 \times 336$  to  $448 \times 448$ . Meanwhile, the MR-Adapter is then applied to connect two visual pathways. Different from the first training stage, the entire MLLM will be fully optimized to better accommodate high-resolution images.

## 5 EXPERIMENTS

### 5.1 EVALUATIONS AND METRICS

**Multimodal benchmarks for MLLM.** We evaluate LLaVA-HR on six emerging multimodal benchmarks for MLLMs, including MME (Fu et al., 2023), POPE (Li et al., 2023c), SEED (Li et al., 2023a), MM-VET (Yu et al., 2023b), MMMU (Yue et al., 2023) and MathVista (Lu et al., 2023). In particular, MME and MM-VET evaluate the multimodal perception and cognition abilities of MLLMs. SEED extends the modalities of evaluation to images and videos. POPE aims to evaluate the visual hallucinations of MLLMs. MMMU and MathVista aim to evaluate the multi-discipline and math understanding ability, respectively. The metrics used in our paper follow their default settings.

**General visual question answering benchmarks.** We also evaluate LLaVA-HR on seven VL datasets, including VQAv2 (Goyal et al., 2017), GQA (Hudson & Manning, 2019), OKVQA (Marino et al., 2019), OCRVQA (Mishra et al., 2019), ScienceQA (Lu et al., 2022a), VizWiz (Gurari et al., 2018) and TextVQA. In particular, ScienceQA (Lu et al., 2022a) and VizWiz (Gurari et al., 2018) are two zero-shot tasks, and their samples are not appeared in our training data. We report the accuracy on the *test* set of OCRVQA, the *test* set of VizWiz, and the *val* set of OKVQA. We organize samples of these tasks in instruction formats of LLaVA-1.5 (Liu et al., 2023a).

**OCR-related benchmarks.** To validate the fine-grained recognition ability of LLaVA-HR, we further evaluate it on five text-rich image understanding tasks, including TextVQA (Singh et al., 2019), DocVQA (Mathew et al., 2021), InfoVQA (Mathew et al., 2022), AI2D (Kembhavi et al., 2016) and ChartVQA (Masry et al., 2022). For DocVQA and InfoVQA, we use the metric of ANLS. For remaining benchmarks, we use the accuracy as the metric. Results of LLaVA-HR on OCR-related benchmarks are evaluated by the VLMEvalKit Duan et al. (2024).

### 5.2 IMPLEMENTATION DETAILS

In LLaVA-HR, we use CLIP-ViT-L (Radford et al., 2021; Ilharco et al., 2021) and CLIP-ConvNeXt-L (Liu et al., 2022) as the dual visual paths to encode low- and high-resolution images, respectively. In LLaVA-HR-X, the CLIP-ConvNeXt-L is replaced with the stronger CLIP-ConvNeXt-XXL. The MR-Adapter is applied into the last three stages of ViT. Following LLaVA-1.5, we first pre-train LLaVA-HR on LCS-558K (Liu et al., 2023b), which contains 558k image-text pairs. During the pre-training stage, both the visual encoder and the LLM are frozen, and only the MLP projector is fine-tuned. AdamW (Kingma & Ba, 2014) is used as the optimizer, and the learning rate and batch size are set to  $1e-3$  and 256, respectively. Visual resolutions are set to  $336 \times 336$  and  $384 \times 384$  for the ViT and the CNN, respectively. During instruction tuning, we follow LLaVA-1.5 to use 665k VL instruction data. When fairly comparing with recent MLLMs like MM1 (McKinzie et al., 2024), we use additional 1.6M instruction data including ShareGPT4V (Chen et al., 2023b), LAION-GPT-4V (laion, 2023), ALLAVA (Chen et al., 2024a), LIMA (Zhou et al., 2024), OpenAssistant2 (Köpf et al., 2024), Tabmwp (Lu et al., 2022b), MathQA (Yu et al., 2023a), KVQA (Shah et al., 2019), Geometry (Lu et al., 2021), STVQA (Biten et al., 2019), ChartQA (Masry et al., 2022), DVQA (Kafle et al., 2018), AI2D (Kembhavi et al., 2016), LLaVA-Med (Li et al., 2024a), InfoVQA (Mathew et al., 2022) and MathV360k Shi et al. (2024). At this stage, the entire model is updated with a learning

Table 1: **Performance and efficiency comparisons of existing high-resolution adaptation solutions.** All experiments are conducted based on LLaVA-1.5. The training and inference costs are measured on NVIDIA A800s. “Res.” and “V-Token” denote image resolutions and the number of visual tokens, respectively. “t/s” denotes the number of generated tokens per second. “N/A” means that GPU memory overflows, so we reduce the batch size.

Methods	Res.	V-Token	Vision-Language Tasks				Training Time ↓	GPU Memory ↓	Inference Speed ↑
			VQAv2	TVQA	MME	POPE			
LLaVA-1.5 (Liu et al., 2023a)	336 pix	576	80.4	59.4	1461	86.2	15.6h	28G	23.8 t/s
+Resize	448 pix	1024	81.1	62.1	1493	87.2	19.4h	49G	19.9 t/s
+Resize	672 pix	2304	81.5	64.2	1498	87.9	31.8h	79G	12.7 t/s
+Resize	1022 pix	5329	74.2	37.8	1266	84.4	69.4h	N/A	5.6 t/s
+Avg. Pooling	756 pix	729	80.6	59.6	1480	86.5	37.3h	45G	23.9 t/s
+CNN Encoder (Liu et al., 2022)	768 pix	576	80.3	64.6	1415	86.6	17.6h	37G	23.7 t/s
+Resampler (Jaegle et al., 2021)	756 pix	64	79.8	58.9	1403	85.8	36.5h	40G	27.6 t/s
+AnyRes (Liu et al., 2024a)	~1088 pix	~2880	81.7	65.1	1487	87.7	33.5h	65G	14.8 t/s
+MRA (ours)	768 pix	576	81.8	64.3	1524	88.0	18.2h	38G	23.5 t/s
+MRA (ours)	1024 pix	1024	81.9	67.1	1554	87.6	20.7h	40G	19.7 t/s

rate of  $2e-5$ . Besides, we increase the resolution of ViT and CNN to  $448 \times 448$  and  $1,024 \times 1,024$ , respectively. The training epoch is set to 1 for pre-training and instruction tuning.

### 5.3 EXPERIMENTAL RESULTS

#### 5.3.1 QUANTITATIVE ANALYSIS

**Comparison with high-resolution baselines.** In Tab. 1, we compare the performance and efficiency of MRA and existing high-resolution solutions on LLaVA-1.5 (Liu et al., 2023a). In this table, “Resize” aims to directly increase the image resolution. “CNN Encoder” replaces the visual backbone with ConvNeXt (Liu et al., 2022), which uses a larger downsampling rate to reduce the number of visual tokens. “Avg. Pooling” and “Resampler” refer to the two pooling strategies for reducing the number of visual tokens. For “Resampler”, we follow QwenVL-Chat and reduce the number of visual tokens to 64. “AnyRes” divides a high-resolution image into several sub-images (Liu et al., 2024a). From this table, we observe that directly increasing image resolution obviously improves the performance of two models on four tasks, *e.g.*, +4.8% of LLaVA-1.5 on TextVQA. However, the performance of LLaVA-1.5 drops significantly at the resolution of  $1,024 \times 1,024$ . To explain, the number of visual tokens greatly exceeds the pre-trained context length of the LLM, which easily causes the instability during training. Besides, we can also see that although several baselines can well maintain the inference efficiency, their benefits to performance are not obvious.

In particular, “Resampler” even hurts the model performance on four benchmark datasets, which often requires large-scale pre-training to achieve a promising performance. In contrast, as the most popular solution in existing literature (Liu et al., 2024a; Gao et al., 2024), “AnyRes” can effectively bring obvious performance gains on TextVQA and POPE. Nevertheless, the number of visual token increases significantly, leading to extremely high computational complexity. Compared to these methods, the performance of MRA is consistently improved from  $768 \times 768$  resolution to  $1,024 \times 1,024$  resolution. Besides, the total gain of MRA is more obvious than that of all compared methods, *e.g.*, +2.0% against AnyRes (Liu et al., 2024a) on TextVQA.

In addition to performance, the expenditure of LLaVA-HR is also cost-effective. In particular, increasing resolution from  $336 \times 336$  to  $1,022 \times 1,022$  slows down the training and inference of

Table 2: **Ablation Study of MRA on LLaVA-1.5.** “Tune vision” means that the image encoder is fine-tuned.

Methods	VQAv2	TVQA	MME	POPE
LLaVA-1.5 (Liu et al., 2023a)	78.5	58.2	1510.7	85.9
+Tune vision	80.4 +0.9	59.4 +1.2	1461.2 -49.5	86.2 +0.3
+Dual-pathway	81.3 +1.8	62.8 +4.6	1513.1 +2.4	87.2 +1.3
+MR-Adapter	81.8 +2.3	64.4 +6.2	1524.8 +14.1	88.0 +2.1
+1024 resolution	81.9 +2.4	67.1 +8.9	1554.9 +44.2	87.6 +1.7
+13B LLM	82.3 +2.8	68.1 +9.9	1540.9 +30.2	87.8 +1.9
+1B Vision	82.6 +3.1	70.9 +12.7	1487.3 -23.4	88.0 +2.1

Table 4: **Comparison with existing methods on four MLLM benchmarks.** “Param.,” “Res.” and “Data” refer to the parameters, the resolution and the training data, respectively. “t/s” refers to tokens per second. CogVLM-Chat and InternVL-1.2 use more data and parameters, so we mark it in gray.

Method	Settings			General MLLM Benchmarks						Inference	
	Param.	Res.	Data	MME	POPE	SEED	SEED <sup>†</sup>	MM-Vet	MMMU	MathVista	Speed
BLIP-2 (Li et al., 2023b)	14B	224	129M	1293.8	85.3	46.4	49.7	22.4	-	-	-
InstructBLIP (Dai et al., 2023)	14B	224	130M	1212.8	78.9	-	-	25.6	-	-	-
QwenVL-Chat (Bai et al., 2023)	10B	448	1.4B	1487.5	-	58.2	65.4	-	35.9	-	17.0 t/s
Fuyu-8B (Fuyu-8B, 2023)	8B	600	-	728.6	74.1	-	-	21.4	-	-	15.6 t/s
mPLUG-Owl2 (Ye et al., 2023)	8B	448	400M	1450.2	-	57.8	-	36.2	32.7	-	19.6 t/s
I-MoF (Tong et al., 2024)	13B	336	1.2M	-	86.7	-	-	34.6	-	-	-
LLaVA-1.5 (Liu et al., 2023a)	7B	336	1.2M	1510.7	85.9	58.6	66.1	30.5	-	-	23.8 t/s
LLaVA-1.5 (Liu et al., 2023a)	13B	336	1.2M	1531.3	85.9	61.6	68.2	35.4	36.4	27.6	16.1 t/s
LLaVA-HR	7B	1024	1.2M	<b>1554.9</b>	87.6	64.2	70.6	31.5	35.2	<b>28.5</b>	19.7 t/s
LLaVA-HR	13B	1024	1.2M	1540.9	87.8	64.5	70.9	35.5	35.7	27.7	15.0 t/s
LLaVA-HR-X	14B	1024	1.2M	1487.3	<b>88.0</b>	<b>65.3</b>	<b>71.4</b>	<b>40.3</b>	<b>36.6</b>	28.1	12.9 t/s
<i>More Instruction Data:</i>											
LLaVA-NeXT (Liu et al., 2024a)	7B	1344	1.6M	1519.0	86.5	-	70.2	43.9	35.8	34.6	14.8 t/s
SPHINX-intern2 (Gao et al., 2024)	7B	448	16M	1260.4	86.9	-	-	36.5	-	35.5	-
InternLM-XC (Zhang et al., 2023)	7B	224	1.1B	1528.4	-	-	-	35.2	-	29.5	-
Mini-Gemini (Li et al., 2024b)	7B	672	2.7M	<b>1546.0</b>	-	-	-	41.3	36.8	32.2	16.2 t/s
MM1 (McKinzie et al., 2024)	7B	1792	1B	1529.3	86.6	64.0	69.9	42.1	37.0	35.9	-
CogVLM-Chat (Wang et al., 2023)	17B	490	1.5B	-	-	-	-	51.1	41.1	34.5	11.5 t/s
InternVL-1.2 (Chen et al., 2023d)	40B	448	450M	1687.0	-	-	-	48.9	51.6	47.7	11.3 t/s
LLaVA-HR†	7B	1024	2.7M	1490.5	<b>86.9</b>	<b>64.9</b>	<b>71.9</b>	<b>45.1</b>	<b>38.4</b>	<b>46.0</b>	19.7 t/s

LLaVA-1.5 by 344.8% and 325%, respectively. However, these costs are reduced to only 17.6% and 20.8% in LLaVA-HR. Despite better performance, the training and inference speeds of LLaVA-HR are three times faster than LLaVA-1.5. Besides, the costs of GPU memory also remain cheap for LLaVA-HR. For example, adapting the resolution of  $1,024 \times 1,024$  for LLaVA-HR only consumes 40G GPU memory, but the same settings for LLaVA-1.5 will cause GPU memory overflow. These results greatly confirm the efficiency of our MRA and LLaVA-HR.

**Ablation studies.** In Tab. 2 and 3, we conduct comprehensive ablation studies for MRA on four benchmarks. Firstly, we validate each design of our MRA in Tab. 2. From these results, we find that each component obviously contributes to the final performance. For example, the dual visual pathways and the MR-Adapter provide +3.4% and +1.6% performance gains on TextVQA, respectively. After increasing the resolution to  $1,024 \times 1,024$ , the performance on TextVQA further boosts by +2.7%. In the second block of Tab. 2, we also ablate the parameter scale of the LLM and the visual encoder. Experimental results show that larger visual backbone or LLM will consistently improve the model performance, further confirming the scalability of MRA.

In Tab 3, we compare different designs in MRA. From these results, we find that a larger high-resolution visual encoder typically brings more gains than a larger low-resolution one. Besides, the fusion direction of MRA is also significant. Specifically, changing the fusion direction obviously degenerates the performance, *e.g.*, -61.3 on MME. Such results also confirm our design principle of MRA, *i.e.*, embedding high-resolution information in to low-resolution pathway. Meanwhile, the best choice of the insert position of MRA is the last 3 stages of ViT. These ablations further confirm the designs of MR-Adapter.

Table 3: **Different choices of MRA on LLaVA-HR.** “L-Res Path.,” “H-Res Path.” and “Fusion Direct.” denote the low-resolution pathway, the high-resolution pathway and the fusion direction, respectively. Our final setting is colored in gray.

Settings	Choices	VQAv2	TVQA	MME	POPE
L-Res Path.	ViT-L	81.8	64.4	1524.8	88.0
	ViT-G	81.7	65.3	1469.7	87.9
H-Res Path.	ConvXt-L	81.8	64.4	1524.8	88.0
	ConvXt-XXL	82.3	66.5	1479.2	87.9
Fusion Direct.	High to Low	81.8	64.4	1524.8	88.0
	Low to High	81.0	62.8	1463.5	87.3
Insert Position	last 3 stages	81.8	64.4	1524.8	88.0
	last stage	81.3	62.8	1513.1	87.2
	last 2 stages	81.6	63.8	1508.4	87.5
	last 4 stages	81.4	63.1	1461.6	87.5

Table 5: Comparison with existing methods on seven general visual question answering tasks. SQA<sup>I</sup> refers to the IMG subset of ScienceQA.

Method	Settings			General Visual Question Answering							Infer. Speed
	Param.	Res.	Data	VQAv2	GQA	OKVQA	OCRVQA	SQA <sup>I</sup>	VizWiz	TVQA	
BLIP-2 (Li et al., 2023b)	14B	224	129M	41.0	41.0	45.9	40.6	61.0	19.6	42.5	-
InstructBLIP (Dai et al., 2023)	14B	224	130M	-	49.5	-	44.8	63.1	33.4	50.7	-
Shikra (Chen et al., 2023a)	13B	224	6.1M	77.4	-	-	-	-	-	-	-
IDEFICS-9B (IDEFICS, 2023)	9B	224	354M	50.9	-	38.4	-	-	35.5	25.9	30.5 t/s
IDEFICS-80B (IDEFICS, 2023)	80B	224	354M	60.0	-	45.2	-	-	36.0	30.9	-
QwenVL-Chat (Bai et al., 2023)	10B	448	1.4B	78.2	57.5	56.6	<b>70.5</b>	68.2	38.9	61.5	17.0 t/s
Fuyu-8B (Fuyu-8B, 2023)	8B	600	-	74.2	-	60.6	-	-	-	-	15.6 t/s
mPLUG-Owl2 (Ye et al., 2023)	8B	448	400M	79.4	56.1	57.7	-	68.7	54.5	58.2	19.6 t/s
I-MoF (Tong et al., 2024)	13B	336	1.2M	79.3	-	-	-	-	-	58.7	-
LLaVA-1.5 (Liu et al., 2023a)	7B	336	1.2M	78.5	62.0	-	-	66.8	50.0	58.2	23.8 t/s
LLaVA-1.5 (Liu et al., 2023a)	13B	336	1.2M	80.0	63.3	-	-	<b>71.6</b>	53.6	61.3	16.1 t/s
LLaVA-HR	7B	1024	1.2M	81.9	64.2	58.9	68.4	67.9	48.7	67.1	19.7 t/s
LLaVA-HR	13B	1024	1.2M	82.3	64.8	60.7	67.7	70.1	<b>57.9</b>	68.1	15.0 t/s
LLaVA-HR-X	14B	1024	1.2M	<b>82.6</b>	<b>65.2</b>	<b>61.5</b>	69.0	69.7	56.6	<b>70.9</b>	12.9 t/s

Table 6: Comparison with existing MLLMs on five multimodal OCR-related benchmarks.

Method	Param.	Res.	Data.	TextVQA	DocVQA	InfoVQA	AI2D	ChartQA
QwenVL (Bai et al., 2023)	10B	336	1.4B	63.8	65.1	35.4	-	65.7
Monkey (Li et al., 2024c)	10B	1344	1.4M	67.6	66.5	36.1	62.6	-
LLaVA-NeXT (Liu et al., 2024a)	7B	1344	1.6M	64.9	-	-	66.6	54.8
TextMonkey (Liu et al., 2024b)	10B	1344	2.5M	65.9	73.0	28.6	-	65.5
DocOwl-1.5-Chat (Hu et al., 2024)	8B	4032	4M	68.6	82.2	50.7	-	70.2
CogAgent Hong et al. (2023)	18B	1120	>300M	<b>76.1</b>	81.6	44.5	-	68.4
LLaVA-HR†	7B	1024	2.7M	73.8	<b>85.8</b>	<b>52.3</b>	<b>75.3</b>	<b>77.6</b>

**Comparison with existing MLLMs.** In Tab. 4 and 5, we compare LLaVA-HR with existing MLLMs on 13 VL tasks. On the six MLLM benchmarks, we observe comprehensive advantages of LLaVA-HR against existing MLLMs. In particular, LLaVA-HR achieves 1554.9 scores in MME benchmark, outperforming LLaVA-1.5 by +23.6. On POPE, a benchmark including video evaluations, LLaVA-HR-X still outperforms existing MLLMs by a large margin, *i.e.*, +3.7% gains. Besides, LLaVA-HR achieves the best performance on the benchmark for visual hallucinations, *i.e.*, POPE, suggesting that its visual hallucinations are greatly alleviated. Meanwhile, we also compare the recently proposed MLLMs in the second block of Tab. 4. In particular, we still observe the better performance of LLaVA-HR against LLaVA-NeXT (Liu et al., 2024a), SPHINX-intern2 (Gao et al., 2024), Mini-Gemini (Li et al., 2024b) and MM1 (McKinzie et al., 2024), *e.g.*, +3.0% on MM-Vet.

Tab. 5 gives the performance comparison on common VL tasks. On in-domain tasks, LLaVA-HR achieves the best results on three tasks, *e.g.*, 82.6 on VQAv2 and 61.5 on OKVQA. On OCRVQA, Qwen-VL-Chat collects more in-domain data for training, so it performs better than LLaVA-HR. Under the zero-shot setting, we can observe more significant advantages of LLaVA-HR on the fine-grained tasks, *e.g.*, VizWiz. Most notably, even Qwen-VL-Chat is pre-trained with 24.8M OCR samples, it still performs worse than LLaVA-HR-X on TextVQA. These results suggest the significance of high resolution for these tasks. In contrast, most images of ScienceQA are synthetic and of low resolution, so the advantages of LLaVA-HR are not obvious. Overall, these results greatly confirm the effectiveness and generalization of LLaVA-HR and our MRA.

Tab. 6 compares LLaVA-HR and existing MLLMs on text-rich image understanding tasks. Compared to common MLLM benchmarks and VQA benchmarks, these OCR-related benchmarks pose a higher requirement for image resolution. As shown in Tab. 6, low-resolution MLLMs like QwenVL often perform inferior to high-resolution ones, *e.g.*, -4.8% on TextVQA compared to DocOwl-1.5-Chat Hu et al. (2024). However, we still observe that LLaVA-HR greatly outperforms existing MLLMs on five benchmarks. For example, although DocOwl-1.5-Chat has larger model size, input resolution and data size, LLaVA-HR also demonstrates superior fine-grained text recognition ability, *e.g.*, +3.6 on DocVQA and +1.6 on InfoVQA. These results further validate the effectiveness of our mixture-of-resolution design on text-rich image understanding tasks.



Figure 4: **Visualizations of LLaVA-HR and existing MLLMs.** Subfig-(a) shows that high image resolution greatly improves the capability of MLLMs on fine-grained VL tasks. In Subfig-(b), LLaVA-HR-X demonstrates the comparable ability with GPT4-V in visual information extraction. Correct and incorrect answers are colored in green and red, respectively.

### 5.3.2 QUALITATIVE EXPERIMENTS

In Fig 4 (a), we compare the predictions of LLaVA-HR with different resolutions. The visualizations show that higher image resolution obviously improves the capability of MLLMs on fine-grained tasks. For example, LLaVA-HR with a resolution of  $1,024 \times 1,024$  can well capture granular visual content, e.g., the tiny boat in the first example. Besides, high image resolution also enables LLaVA-HR a stronger ability of text recognition. For instance, the small and blurred phrase of “wo ich wohne” in the second example are correctly identified by the high-resolution LLaVA-HR. These results greatly confirm the significance of high image resolution in addressing visual shortcoming. In Fig 4 (b), we further compare the predictions of LLaVA-HR-X, LLaVA-1.5 (Liu et al., 2023a) and GPT4-V (OpenAI, 2023) in visual information extraction. Notably, LLaVA-HR-X shows a comparable ability with GPT4-V on this challenging task. As shown in Fig 4 (b), LLaVA-HR-X and GPT4-V can correctly extract almost all visual content of the driver license and organize it in JSON format. Compared to GPT4-V, LLaVA-HR-X also correctly identifies the hair color of the person, which requires fine-grained visual reasoning. In contrast, LLaVA-1.5 can only recognize simple visual content like “class” and “SEX”, and fail to extract most visual information. These results further validate the effectiveness of MRA in addressing visual shortcoming of MLLMs.

## 6 CONCLUSION

In this paper, we focus on the efficient high-resolution adaptation for MLLMs and propose a novel method, namely *mixture-of-resolution adaptation* (MRA). MRA adopts dual visual pathways to process images of both high and low resolutions, where high-resolution information is embedded into the low-resolution modeling via the novel *mixture-of-resolution adapters* (MR-Adapters). We apply MRA to a popular MLLM called LLaVA-1.5, and construct a new high-resolution MLLM, termed LLaVA-HR. Experimental results not only validate the effectiveness of LLaVA-HR in addressing visual shortcoming, but also confirm its remarkable efficiency against existing MLLMs.

**Acknowledgments.** This work was supported by the National Science Fund for Distinguished Young Scholars (No.62025603), the China Postdoctoral Science Foundation (No. 2024M761548), the National Natural Science Foundation of China (No. U21B2037, No. U22B2051, No. 623B2088, No. U23A20383, No. U21A20472, No. 62176222, No. 62176223, No. 62176226, No. 62072386, No. 62072387, No. 62072389, No. 62002305 and No. 62272401), the Natural Science Foundation of Fujian Province of China (No. 2021J06003, No.2022J06001) and the Fundamental Research Funds for the Central Universities (Xiamen University: No. 20720240053).

## REFERENCES

- Jean-Baptiste Alayrac, Jeff Donahue, Pauline Luc, Antoine Miech, Iain Barr, Yana Hasson, Karel Lenc, Arthur Mensch, Katie Millican, Malcolm Reynolds, et al. Flamingo: a visual language model for few-shot learning. *arXiv preprint arXiv:2204.14198*, 2022.
- Jinze Bai, Shuai Bai, Shusheng Yang, Shijie Wang, Sinan Tan, Peng Wang, Junyang Lin, Chang Zhou, and Jingren Zhou. Qwen-vl: A frontier large vision-language model with versatile abilities. *arXiv preprint arXiv:2308.12966*, 2023.
- Ali Furkan Biten, Ruben Tito, Andres Mafla, Lluís Gomez, Marçal Rusinol, Ernest Valveny, CV Jawahar, and Dimosthenis Karatzas. Scene text visual question answering. In *Proceedings of the IEEE/CVF international conference on computer vision*, pp. 4291–4301, 2019.
- Chun-Fu Richard Chen, Quanfu Fan, and Rameswar Panda. Crossvit: Cross-attention multi-scale vision transformer for image classification. In *Proceedings of the IEEE/CVF international conference on computer vision*, pp. 357–366, 2021.
- Guiming Hardy Chen, Shunian Chen, Ruifei Zhang, Junying Chen, Xiangbo Wu, Zhiyi Zhang, Zhihong Chen, Jianquan Li, Xiang Wan, and Benyou Wang. Allava: Harnessing gpt4v-synthesized data for a lite vision-language model. *arXiv preprint arXiv:2402.11684*, 2024a.
- Keqin Chen, Zhao Zhang, Weili Zeng, Richong Zhang, Feng Zhu, and Rui Zhao. Shikra: Unleashing multimodal llm’s referential dialogue magic. *arXiv preprint arXiv:2306.15195*, 2023a.
- Lin Chen, Jisong Li, Xiaoyi Dong, Pan Zhang, Conghui He, Jiaqi Wang, Feng Zhao, and Dahua Lin. Sharegpt4v: Improving large multi-modal models with better captions. *arXiv preprint arXiv:2311.12793*, 2023b.
- Ting Chen, Simon Kornblith, Kevin Swersky, Mohammad Norouzi, and Geoffrey E Hinton. Big self-supervised models are strong semi-supervised learners. *Advances in neural information processing systems (NeurIPS)*, 33:22243–22255, 2020.
- Xi Chen, Xiao Wang, Soravit Changpinyo, AJ Piergiovanni, Piotr Padlewski, Daniel Salz, Sebastian Goodman, Adam Grycner, Basil Mustafa, Lucas Beyer, et al. Pali: A jointly-scaled multilingual language-image model. *arXiv preprint arXiv:2209.06794*, 2022.
- Xi Chen, Xiao Wang, Lucas Beyer, Alexander Kolesnikov, Jialin Wu, Paul Voigtlaender, Basil Mustafa, Sebastian Goodman, Ibrahim Alabdulmohsin, Piotr Padlewski, et al. Pali-3 vision language models: Smaller, faster, stronger. *arXiv preprint arXiv:2310.09199*, 2023c.
- Zhe Chen, Jiannan Wu, Wenhai Wang, Weijie Su, Guo Chen, Sen Xing, Zhong Muyan, Qinglong Zhang, Xizhou Zhu, Lewei Lu, et al. Internvl: Scaling up vision foundation models and aligning for generic visual-linguistic tasks. *arXiv preprint arXiv:2312.14238*, 2023d.
- Zhe Chen, Weiyun Wang, Hao Tian, Shenglong Ye, Zhangwei Gao, Erfei Cui, Wenwen Tong, Kongzhi Hu, Jiapeng Luo, Zheng Ma, et al. How far are we to gpt-4v? closing the gap to commercial multimodal models with open-source suites. *arXiv preprint arXiv:2404.16821*, 2024b.
- Wenliang Dai, Junnan Li, Dongxu Li, Anthony Meng Huat Tiong, Junqi Zhao, Weisheng Wang, Boyang Li, Pascale Fung, and Steven Hoi. Instructblip: Towards general-purpose vision-language models with instruction tuning. *arXiv preprint arXiv:2305.06500*, 2023.

- Xiaoyi Dong, Pan Zhang, Yuhang Zang, Yuhang Cao, Bin Wang, Linke Ouyang, Songyang Zhang, Haodong Duan, Wenwei Zhang, Yining Li, et al. Internlm-xcomposer2-4khd: A pioneering large vision-language model handling resolutions from 336 pixels to 4k hd. *arXiv preprint arXiv:2404.06512*, 2024.
- Alexey Dosovitskiy, Lucas Beyer, Alexander Kolesnikov, Dirk Weissenborn, Xiaohua Zhai, Thomas Unterthiner, Mostafa Dehghani, Matthias Minderer, Georg Heigold, Sylvain Gelly, et al. An image is worth 16x16 words: Transformers for image recognition at scale. *arXiv preprint arXiv:2010.11929*, 2020.
- Haodong Duan, Junming Yang, Yuxuan Qiao, Xinyu Fang, Lin Chen, Yuan Liu, Xiaoyi Dong, Yuhang Zang, Pan Zhang, Jiaqi Wang, Dahua Lin, and Kai Chen. Vlmevalkit: An open-source toolkit for evaluating large multi-modality models, 2024. URL <https://arxiv.org/abs/2407.11691>.
- Chaoyou Fu, Peixian Chen, Yunhang Shen, Yulei Qin, Mengdan Zhang, Xu Lin, Zhenyu Qiu, Wei Lin, Jinrui Yang, Xiawu Zheng, et al. Mme: A comprehensive evaluation benchmark for multimodal large language models. *arXiv preprint arXiv:2306.13394*, 2023.
- Fuyu-8B. <https://www.adept.ai/blog/fuyu-8b>, 2023.
- Peng Gao, Renrui Zhang, Chris Liu, Longtian Qiu, Siyuan Huang, Weifeng Lin, Shitian Zhao, Shijie Geng, Ziyi Lin, Peng Jin, et al. Sphinx-x: Scaling data and parameters for a family of multi-modal large language models. *arXiv preprint arXiv:2402.05935*, 2024.
- Fabrizio Gilardi, Meysam Alizadeh, and Maël Kubli. Chatgpt outperforms crowd-workers for text-annotation tasks. *arXiv preprint arXiv:2303.15056*, 2023.
- Yash Goyal, Tejas Khot, Douglas Summers-Stay, Dhruv Batra, and Devi Parikh. Making the v in vqa matter: Elevating the role of image understanding in visual question answering. In *Proceedings of the IEEE conference on computer vision and pattern recognition*, pp. 6904–6913, 2017.
- Danna Gurari, Qing Li, Abigale J Stangl, Anhong Guo, Chi Lin, Kristen Grauman, Jiebo Luo, and Jeffrey P Bigham. Vizwiz grand challenge: Answering visual questions from blind people. In *Proceedings of the IEEE conference on computer vision and pattern recognition*, pp. 3608–3617, 2018.
- Wenyi Hong, Weihang Wang, Qingsong Lv, Jiazheng Xu, Wenmeng Yu, Junhui Ji, Yan Wang, Zihan Wang, Yuxiao Dong, Ming Ding, and Jie Tang. Cogagent: A visual language model for gui agents, 2023.
- Anwen Hu, Haiyang Xu, Jiabo Ye, Ming Yan, Liang Zhang, Bo Zhang, Chen Li, Ji Zhang, Qin Jin, Fei Huang, et al. mplug-docowl 1.5: Unified structure learning for ocr-free document understanding. *arXiv preprint arXiv:2403.12895*, 2024.
- Drew A Hudson and Christopher D Manning. Gqa: A new dataset for real-world visual reasoning and compositional question answering. In *CVPR*, 2019.
- IDEFICS. Introducing idefics: An open reproduction of state-of-the-art visual language model. <https://huggingface.co/blog/idefics>, 2023.
- Gabriel Ilharco, Mitchell Wortsman, Ross Wightman, Cade Gordon, Nicholas Carlini, Rohan Taori, Achal Dave, Vaishaal Shankar, Hongseok Namkoong, John Miller, Hannaneh Hajishirzi, Ali Farhadi, and Ludwig Schmidt. Openclip. July 2021. doi: 10.5281/zenodo.5143773. URL <https://doi.org/10.5281/zenodo.5143773>. If you use this software, please cite it as below.
- Andrew Jaegle, Felix Gimeno, Andy Brock, Oriol Vinyals, Andrew Zisserman, and Joao Carreira. Perceiver: General perception with iterative attention. In *International conference on machine learning*, pp. 4651–4664. PMLR, 2021.
- Huaizu Jiang, Ishan Misra, Marcus Rohrbach, Erik Learned-Miller, and Xinlei Chen. In defense of grid features for visual question answering. In *Proceedings of the IEEE/CVF conference on computer vision and pattern recognition*, pp. 10267–10276, 2020.

- Kushal Kafle, Brian Price, Scott Cohen, and Christopher Kanan. Dvqa: Understanding data visualizations via question answering. In *Proceedings of the IEEE conference on computer vision and pattern recognition*, pp. 5648–5656, 2018.
- Aniruddha Kembhavi, Mike Salvato, Eric Kolve, Minjoon Seo, Hannaneh Hajishirzi, and Ali Farhadi. A diagram is worth a dozen images. In *Computer Vision–ECCV 2016: 14th European Conference, Amsterdam, The Netherlands, October 11–14, 2016, Proceedings, Part IV 14*, pp. 235–251. Springer, 2016.
- Diederik P Kingma and Jimmy Ba. Adam: A method for stochastic optimization. *arXiv preprint arXiv:1412.6980*, 2014.
- Andreas Köpf, Yannic Kilcher, Dimitri von Rütte, Sotiris Anagnostidis, Zhi Rui Tam, Keith Stevens, Abdullah Barhoum, Duc Nguyen, Oliver Stanley, Richard Nagyfi, et al. Openassistant conversations-democratizing large language model alignment. *Advances in Neural Information Processing Systems*, 36, 2024.
- laion. laion gpt4v. <https://huggingface.co/datasets/laion/gpt4v-dataset>, 2023.
- Bohao Li, Rui Wang, Guangzhi Wang, Yuying Ge, Yixiao Ge, and Ying Shan. Seed-bench: Benchmarking multimodal llms with generative comprehension. *arXiv preprint arXiv:2307.16125*, 2023a.
- Chunyu Li, Cliff Wong, Sheng Zhang, Naoto Usuyama, Haotian Liu, Jianwei Yang, Tristan Naumann, Hoifung Poon, and Jianfeng Gao. Llava-med: Training a large language-and-vision assistant for biomedicine in one day. *Advances in Neural Information Processing Systems*, 36, 2024a.
- Junnan Li, Dongxu Li, Silvio Savarese, and Steven Hoi. Blip-2: Bootstrapping language-image pre-training with frozen image encoders and large language models. *arXiv preprint arXiv:2301.12597*, 2023b.
- Yanwei Li, Yuechen Zhang, Chengyao Wang, Zhisheng Zhong, Yixin Chen, Ruihang Chu, Shaoteng Liu, and Jiaya Jia. Mini-gemini: Mining the potential of multi-modality vision language models. *arXiv preprint arXiv:2403.18814*, 2024b.
- Yifan Li, Yifan Du, Kun Zhou, Jinpeng Wang, Wayne Xin Zhao, and Ji-Rong Wen. Evaluating object hallucination in large vision-language models. *arXiv preprint arXiv:2305.10355*, 2023c.
- Zhang Li, Biao Yang, Qiang Liu, Zhiyin Ma, Shuo Zhang, Jingxu Yang, Yabo Sun, Yuliang Liu, and Xiang Bai. Monkey: Image resolution and text label are important things for large multi-modal models. In *Proceedings of the IEEE/CVF Conference on Computer Vision and Pattern Recognition*, pp. 26763–26773, 2024c.
- Haotian Liu, Chunyu Li, Yuheng Li, and Yong Jae Lee. Improved baselines with visual instruction tuning. *arXiv preprint arXiv:2310.03744*, 2023a.
- Haotian Liu, Chunyu Li, Qingyang Wu, and Yong Jae Lee. Visual instruction tuning. In *NeurIPS*, 2023b.
- Haotian Liu, Chunyu Li, Yuheng Li, Bo Li, Yuanhan Zhang, Sheng Shen, and Yong Jae Lee. Llava-next: Improved reasoning, ocr, and world knowledge, January 2024a. URL <https://llava-vl.github.io/blog/2024-01-30-llava-next/>.
- Yuliang Liu, Biao Yang, Qiang Liu, Zhang Li, Zhiyin Ma, Shuo Zhang, and Xiang Bai. Textmonkey: An ocr-free large multimodal model for understanding document. *arXiv preprint arXiv:2403.04473*, 2024b.
- Zhuang Liu, Hanzi Mao, Chao-Yuan Wu, Christoph Feichtenhofer, Trevor Darrell, and Saining Xie. A convnet for the 2020s. In *Proceedings of the IEEE/CVF conference on computer vision and pattern recognition*, pp. 11976–11986, 2022.

- Jiasen Lu, Dhruv Batra, Devi Parikh, and Stefan Lee. Vilbert: Pretraining task-agnostic visiolinguistic representations for vision-and-language tasks. *arXiv preprint arXiv:1908.02265*, 2019.
- Pan Lu, Ran Gong, Shibiao Jiang, Liang Qiu, Siyuan Huang, Xiaodan Liang, and Song-Chun Zhu. Inter-gps: Interpretable geometry problem solving with formal language and symbolic reasoning. *arXiv preprint arXiv:2105.04165*, 2021.
- Pan Lu, Swaroop Mishra, Tanglin Xia, Liang Qiu, Kai-Wei Chang, Song-Chun Zhu, Oyvind Tafjord, Peter Clark, and Ashwin Kalyan. Learn to explain: Multimodal reasoning via thought chains for science question answering. *Advances in Neural Information Processing Systems*, 2022a.
- Pan Lu, Liang Qiu, Kai-Wei Chang, Ying Nian Wu, Song-Chun Zhu, Tanmay Rajpurohit, Peter Clark, and Ashwin Kalyan. Dynamic prompt learning via policy gradient for semi-structured mathematical reasoning. *arXiv preprint arXiv:2209.14610*, 2022b.
- Pan Lu, Hritik Bansal, Tony Xia, Jiacheng Liu, Chunyuan Li, Hannaneh Hajishirzi, Hao Cheng, Kai-Wei Chang, Michel Galley, and Jianfeng Gao. Mathvista: Evaluating mathematical reasoning of foundation models in visual contexts. *arXiv preprint arXiv:2310.02255*, 2023.
- Gen Luo, Yiyi Zhou, Tianhe Ren, Shengxin Chen, Xiaoshuai Sun, and Rongrong Ji. Cheap and quick: Efficient vision-language instruction tuning for large language models. *Advances in neural information processing systems (NeurIPS)*, 2023.
- Gen Luo, Xue Yang, Wenhan Dou, Zhaokai Wang, Jifeng Dai, Yu Qiao, and Xizhou Zhu. Mono-intervl: Pushing the boundaries of monolithic multimodal large language models with endogenous visual pre-training. *arXiv preprint arXiv:2410.08202*, 2024a.
- Yaxin Luo, Gen Luo, Jiayi Ji, Yiyi Zhou, Xiaoshuai Sun, Zhiqiang Shen, and Rongrong Ji.  $\gamma$ -mod: Exploring mixture-of-depth adaptation for multimodal large language models. *arXiv preprint arXiv:2410.13859*, 2024b.
- Kenneth Marino, Mohammad Rastegari, Ali Farhadi, and Roozbeh Mottaghi. Ok-vqa: A visual question answering benchmark requiring external knowledge. In *Conference on Computer Vision and Pattern Recognition (CVPR)*, 2019.
- Ahmed Masry, Do Xuan Long, Jia Qing Tan, Shafiq Joty, and Enamul Hoque. Chartqa: A benchmark for question answering about charts with visual and logical reasoning. *arXiv preprint arXiv:2203.10244*, 2022.
- Minesh Mathew, Dimosthenis Karatzas, and CV Jawahar. Docvqa: A dataset for vqa on document images. In *Proceedings of the IEEE/CVF winter conference on applications of computer vision*, pp. 2200–2209, 2021.
- Minesh Mathew, Viraj Bagal, Rubèn Tito, Dimosthenis Karatzas, Ernest Valveny, and CV Jawahar. Infographicvqa. In *Proceedings of the IEEE/CVF Winter Conference on Applications of Computer Vision*, pp. 1697–1706, 2022.
- Brandon McKinzie, Zhe Gan, Jean-Philippe Fauconnier, Sam Dodge, Bowen Zhang, Philipp Dufer, Dhruvi Shah, Xianzhi Du, Futang Peng, Floris Weers, et al. Mm1: Methods, analysis & insights from multimodal llm pre-training. *arXiv preprint arXiv:2403.09611*, 2024.
- William H Merigan and John HR Maunsell. How parallel are the primate visual pathways? *Annual review of neuroscience*, 16(1):369–402, 1993.
- Anand Mishra, Shashank Shekhar, Ajeet Kumar Singh, and Anirban Chakraborty. Ocr-vqa: Visual question answering by reading text in images. In *2019 international conference on document analysis and recognition (ICDAR)*, pp. 947–952. IEEE, 2019.
- OpenAI. Gpt-4v(ision) system card. [https://cdn.openai.com/papers/GPTV\\_System\\_Card.pdf](https://cdn.openai.com/papers/GPTV_System_Card.pdf), 2023.
- Zhiliang Peng, Wei Huang, Shanzhi Gu, Lingxi Xie, Yaowei Wang, Jianbin Jiao, and Qixiang Ye. Conformer: Local features coupling global representations for visual recognition. In *Proceedings of the IEEE/CVF international conference on computer vision*, pp. 367–376, 2021.

- Zhiliang Peng, Wenhui Wang, Li Dong, Yaru Hao, Shaohan Huang, Shuming Ma, and Furu Wei. Kosmos-2: Grounding multimodal large language models to the world. *arXiv preprint arXiv:2306.14824*, 2023.
- Alec Radford, Jong Wook Kim, Chris Hallacy, Aditya Ramesh, Gabriel Goh, Sandhini Agarwal, Girish Sastry, Amanda Askell, Pamela Mishkin, Jack Clark, et al. Learning transferable visual models from natural language supervision. *arXiv preprint arXiv:2103.00020*, 2021.
- Lynn C Robertson and Marvin R Lamb. Neuropsychological contributions to theories of part/whole organization. *Cognitive psychology*, 23(2):299–330, 1991.
- Daniel Rose, Vaishnavi Himakunthala, Andy Ouyang, Ryan He, Alex Mei, Yujie Lu, Michael Saxon, Chinmay Sonar, Diba Mirza, and William Yang Wang. Visual chain of thought: Bridging logical gaps with multimodal infillings. *arXiv preprint arXiv:2305.02317*, 2023.
- Sanket Shah, Anand Mishra, Naganand Yadati, and Partha Pratim Talukdar. Kvqa: Knowledge-aware visual question answering. In *Proceedings of the AAAI conference on artificial intelligence*, volume 33, pp. 8876–8884, 2019.
- Wenhao Shi, Zhiqiang Hu, Yi Bin, Junhua Liu, Yang Yang, See-Kiong Ng, Lidong Bing, and Roy Ka-Wei Lee. Math-llava: Bootstrapping mathematical reasoning for multimodal large language models. *arXiv preprint arXiv:2406.17294*, 2024.
- Amanpreet Singh, Vivek Natarajan, Meet Shah, Yu Jiang, Xinlei Chen, Dhruv Batra, Devi Parikh, and Marcus Rohrbach. Towards vqa models that can read. In *Proceedings of the IEEE/CVF conference on computer vision and pattern recognition*, pp. 8317–8326, 2019.
- Shengbang Tong, Zhuang Liu, Yuexiang Zhai, Yi Ma, Yann LeCun, and Saining Xie. Eyes wide shut? exploring the visual shortcomings of multimodal llms. *arXiv preprint arXiv:2401.06209*, 2024.
- Hugo Touvron, Thibaut Lavril, Gautier Izacard, Xavier Martinet, Marie-Anne Lachaux, Timothée Lacroix, Baptiste Rozière, Naman Goyal, Eric Hambro, Faisal Azhar, et al. Llama: Open and efficient foundation language models. *arXiv preprint arXiv:2302.13971*, 2023.
- Ashish Vaswani, Noam Shazeer, Niki Parmar, Jakob Uszkoreit, Llion Jones, Aidan N Gomez, Łukasz Kaiser, and Illia Polosukhin. Attention is all you need. In *NeurIPS*, 2017.
- Weihan Wang, Qingsong Lv, Wenmeng Yu, Wenyi Hong, Ji Qi, Yan Wang, Junhui Ji, Zhuoyi Yang, Lei Zhao, Xixuan Song, et al. Cogvlm: Visual expert for pretrained language models. *arXiv preprint arXiv:2311.03079*, 2023.
- Qinghao Ye, Haiyang Xu, Jiabo Ye, Ming Yan, Haowei Liu, Qi Qian, Ji Zhang, Fei Huang, and Jingren Zhou. mplug-owl2: Revolutionizing multi-modal large language model with modality collaboration. *arXiv preprint arXiv:2311.04257*, 2023.
- Jun Yu, Jing Li, Zhou Yu, and Qingming Huang. Multimodal transformer with multi-view visual representation for image captioning. *IEEE transactions on circuits and systems for video technology*, 30(12):4467–4480, 2019.
- Longhui Yu, Weisen Jiang, Han Shi, Jincheng Yu, Zhengying Liu, Yu Zhang, James T Kwok, Zhenguo Li, Adrian Weller, and Weiyang Liu. Metamath: Bootstrap your own mathematical questions for large language models. *arXiv preprint arXiv:2309.12284*, 2023a.
- Weihao Yu, Zhengyuan Yang, Linjie Li, Jianfeng Wang, Kevin Lin, Zicheng Liu, Xinchao Wang, and Lijuan Wang. Mm-vet: Evaluating large multimodal models for integrated capabilities. *arXiv preprint arXiv:2308.02490*, 2023b.
- Xiang Yue, Yuansheng Ni, Kai Zhang, Tianyu Zheng, Ruoqi Liu, Ge Zhang, Samuel Stevens, Dongfu Jiang, Weiming Ren, Yuxuan Sun, et al. Mmmu: A massive multi-discipline multimodal understanding and reasoning benchmark for expert agi. *arXiv preprint arXiv:2311.16502*, 2023.

Pan Zhang, Xiaoyi Dong Bin Wang, Yuhang Cao, Chao Xu, Linke Ouyang, Zhiyuan Zhao, Shuangrui Ding, Songyang Zhang, Haodong Duan, Hang Yan, et al. Internlm-xcomposer: A vision-language large model for advanced text-image comprehension and composition. *arXiv preprint arXiv:2309.15112*, 2023.

Pengchuan Zhang, Xiujun Li, Xiaowei Hu, Jianwei Yang, Lei Zhang, Lijuan Wang, Yejin Choi, and Jianfeng Gao. Vinvl: Revisiting visual representations in vision-language models. In *CVPR*, 2021.

Chunting Zhou, Pengfei Liu, Puxin Xu, Srinivasan Iyer, Jiao Sun, Yuning Mao, Xuezhe Ma, Avia Efrat, Ping Yu, Lili Yu, et al. Lima: Less is more for alignment. *Advances in Neural Information Processing Systems*, 36, 2024.

Deyao Zhu, Jun Chen, Xiaoqian Shen, Xiang Li, and Mohamed Elhoseiny. Minigt-4: Enhancing vision-language understanding with advanced large language models. *arXiv preprint arXiv:2304.10592*, 2023.